applied sciences

MDPI

Essay

Case Study of an Underpinning Pile Foundation for an Interval Tunnel Crossing an Existing Bridge

Yuhang Zhou, Yuanming Liu *, Qingzhi Chen, Xun Ou and Yingxiao Li

College of Civil Engineering, Guizhou University, Guiyang 550025, China
* Correspondence: liuym_2021@163.com; Tel.: +86-136-485-063-68

Abstract: When urban subway tunnels cross existing bridge pile foundations, having a pile foundation underpinning that ensures the safe operation of existing bridges while enabling the safe construction of subway tunnels is the focus of attention. This paper takes the running tunnel project from Huaguoyuan West Station to Huaguoyuan East Station of Rail Transit Line 3 in Guiyang City, Guizhou Province as the background. The reasonableness and feasibility of the passive underpinning construction scheme for the Guihuang Viaduct was studied. The construction plan includes the following steps: underpinning pile construction, foundation pit excavation, the concreting of the underpinning bearing platform, and existing pile truncation. In order to ensure the structural safety of the existing viaduct during the construction of the pile foundation underpinning, a 3D numerical model of the construction of pile foundation underpinning and the whole process of tunnel construction was established. The settlement calculation results of the foundation pit and bridge pier were compared and analyzed with the field monitoring data to verify the accuracy of the numerical model. Further detailed analysis of the settlement of the bridge deck, the deformation of the existing piles, the axial forces of the existing piles, and the forces on the underpinning bearing platform was carried out. The results show that the bridge superstructure load can be transferred to the underpinning bearing platform smoothly after the existing pile truncation construction. The removal of obstacle piles during tunnel excavation has a very limited impact on the superstructure of the bridge, proving the reasonableness and feasibility of the construction plan.

Keywords: passive underpinning; interval tunnel crossing excavation; numerical simulation; field monitoring

check for updates

Citation: Zhou, Y.; Liu, Y.; Chen, Q.; Ou, X.; Li, Y. Case Study of an Underpinning Pile Foundation for an Interval Tunnel Crossing an Existing Bridge. *Appl. Sci.* **2022**, *12*, 12566. https://doi.org/10.3390/app122412566

Academic Editors: Zhongsheng Tan and Xiuying Wang

Received: 13 October 2022
Accepted: 3 December 2022
Published: 8 December 2022

1. Introduction

With the development of urban rail transit and underground tunnel engineering in China, tunnel engineering has gained popularity as an effective way to relieve the pressure of surface traffic. During the construction process of a large number of urban tunnels, there will be situations where construction will need to be carried out through the bottom foundation of an existing building or bridge. Pile foundation underpinning technology is often used in engineering to ensure the safety of the original superstructure in the construction process, specifically referring to the expansion of the foundation of existing buildings or foundation reinforcement. In particular, research on tunnel underpass bridge pile foundations has been a hot topic in recent years [1].

Previous studies on pile foundation underpinning have focused on theoretical empirical formulations [2–6], indoor similar model tests [7–12], and numerical simulations [13–19]. Specifically, Shan [2] proposed a new excavation scheme for urban high-rise buildings, and the theoretical equations of lateral frictional resistance and end resistance of existing piles influenced by adjacent boreholes were derived. Liang [3] developed a computational model for the effect of foundation pits on the dynamic impedance of supported piles, considering the effect of stress history. Zhu [7] conducted indoor model tests based on the pile foundation underpinning design scheme. The changes in existing piles and underpinning piles (pile vertical displacement, pile axial force, and lateral friction resistance) before and after underpinning were studied. Wang [10] simulated the construction process by indoor model tests, studying the pile foundation underpinning the construction process and the pile bearing characteristics. Li [13] used a three-dimensional finite element method to compare and analyze the effectiveness of the protection scheme in mitigating the impact of tunnel excavation on the adjacent group piles. The results show that the pile foundation underpinning scheme is effective in reducing the structural settlement and ground deformation of the bridge. Song [16] detailed the key technologies for pile foundation underpinning construction in tunnels, and conducted theoretical analysis, numerical calculation, and field monitoring to verify the reasonableness of the method. Wang [19] used the engineering example of a double-line shield tunnel crossing Fengqi Bridge in Hangzhou Metro Line 2, discussed strengthening options for Fengqi Bridge, and analyzed the monitoring data before and after the shield crossed the bridge.

There have also been many studies on underpinning structural load-bearing systems. Xu [20] used the beam wrapped pile cap method for pile foundation underpinning construction. Due to the limited technical conditions at that time, the effect of the connection between the old and new concrete after its construction could not be effectively monitored. He [21] concluded that the passive pile foundation underpinning project is feasible and reasonable when applied in an eight-story frame structure building. Xu [22] used numerical simulation and theoretical derivation to investigate the reasonable excavation exposure length of pile foundations during the construction of pile foundation underpinning, the force conversion mechanism of a piled raft system, and the influence of shield cut piles on the superstructure. Zhang [23] used underpinning beams as the underpinning structural load-bearing system; at the same time, in order to prevent the cracking of the underpinning bearing platform concrete, several prestressing steel strands were placed inside it. Zhang [24] used an underpinning beam as a load-bearing structure for the underpinning structure. Numerical simulations of pile foundation underpinning construction and tunnel crossing construction processes were carried out using finite element software. Xu [25] used the foundation reinforcement and raft construction of the pile foundation underpinning technique and verified the feasibility of the construction plan by using numerical simulation. Li [26] used an underpinning beam as a construction method for underpinning structures, studied the mechanism of stress transfer during the construction of pile foundation underpinning, and investigated the impact of shield tunnel construction on the stability of pile foundations.

In general, the existing papers on bridge substructure pile foundation underpinning have the following two characteristics: the underpinning structural load-bearing system mainly adopts a raft structure, beam structure, and prestressed beam structure, and the pile foundation underpinning technology mostly adopts the form of active underpinning (using jacking to control the bridge superstructure deformation). There are not many research results on the pile foundation underpinning of bridge substructures using passive underpinning and the underpinning pile cap as the underpinning structural load-bearing system, and no systematic feasibility evaluation has yet been conducted. In this paper, based on previous related studies, we use Midas GTS software to establish a simulation of the entire construction phase, conduct detailed analysis of the mechanical properties of underpinning structures at different construction stages of pile foundation underpinning, and by comparison with the actual monitoring data, the reasonableness and feasibility of the construction plan are verified.

2. Project Overview

2.1. Engineering Background

In Guiyang City, Guizhou Province, the Rail Transit Line 3 phase 1 project takes the following route from Huaguoyuan West Station to Huaguoyuan East Station: the interval tunnel out of Huaguoyuan West Station through the lion rock mountain, undercrossing the school, Guihuang elevated bridge, Chuanqian Railway roadbed, sidecrossing the

Guiguang High-speed Railway bridge pile, undercrossing the Zunyi Middle Road antislip pile and concert hall, and finally arriving at Huaguoyuan East Station. The interval mileage of the piled section under the Guihuang Viaduct is YDK29+255~YDK29+290, ZDK29+280~ZDK29+315. The geographical location of the pile foundation underpinning is shown in Figure 1.

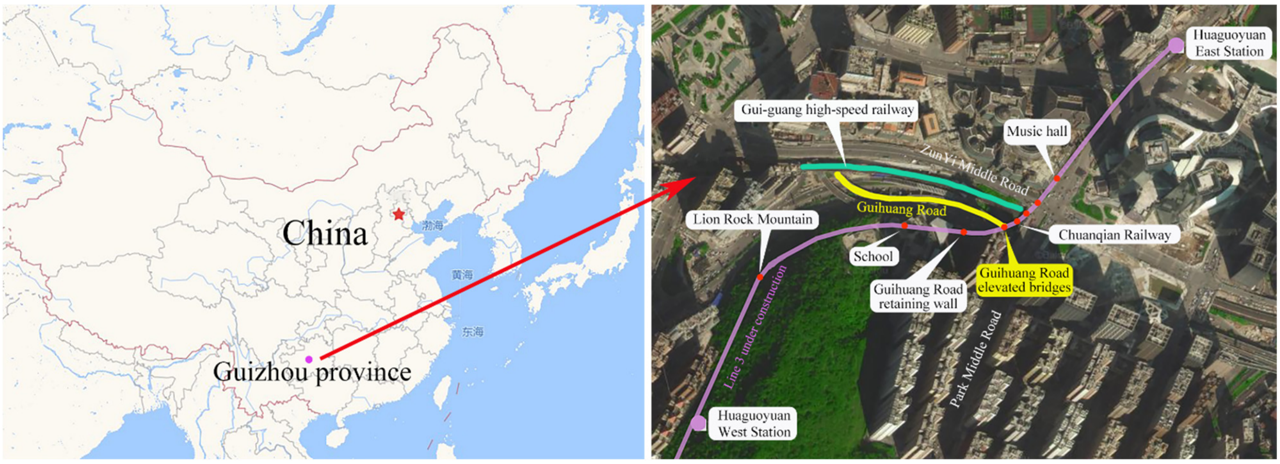

Figure 1. Geographical location of the underpinned pile foundation (Chinese name of the place in the picture).

The tunnel is a horseshoe-shaped single-hole double-line tunnel, and the surrounding rock level of this section of the tunnel is level III, using the upper and lower steps alongside the core soil method of construction. The tunnel is 6.52 m wide and 7.17 m high, and has a double-line spacing of approximately 15 m and a tunnel burial depth of approximately 8.5 m. The tunnel cross section is shown in Figure 2.

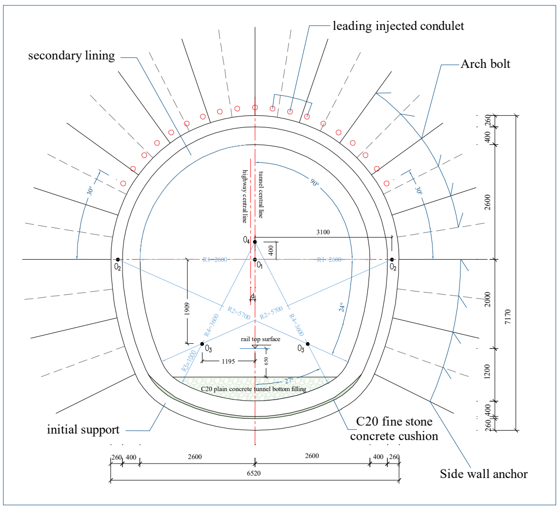

Figure 2. Tunnel cross section.

Guihuang Viaduct is located west of the intersection of Zunyi Middle Road and Park Middle Road, on the north side of Guihuang Road. The bridge is a bidirectional eight-lane reinforced concrete continuous box girder bridge. The girder height is 1.4 m, and the width of the bridge deck varies with the road curve; the cover beam is 1.8 m (height) × 1.6 m (width); the bridge pier is a 1.5 m × 1.5 m square pile and is 7.7 m long; and the old bearing platform is a 7.5 m (length) × 3 m (width) × 2.5 m (height) rectangular bearing platform.

2.2. Engineering Geological Conditions

The interdistrict tunnel at the pile foundation underpinning belongs to a mound and valley landform of the dissolution type. According to the engineering geologic investigation report, the main strata at the pile foundation underpinning are miscellaneous fill, plastic red clay, and medium-weathered limestone. The uppermost layer is <1–2> miscellaneous fill (Q4ml), mainly composed of construction waste and artificial backfilled gravel, etc. The gravel blocks are mainly dolomite, the voids are filled by clayey soil, and the structure is looser. The middle layer is <4–1–3> plastic red clay (Q4el+dl); the soil is brownish-yellow, maroon, etc., and is locally distributed in the stratum, with engineering properties such as softening in water, fissure development, and easy flaking. The lower layer is <20–2–3> medium-weathered limestone (P1m), with a greenish gray, gray-black, medium-layered structure. The rock is relatively complete, and the mineral composition is mainly composed of calcite and biological debris.

To determine the deformation modulus of the rock formation, we conducted an indoor rock test, as shown in Figure 3. The uniaxial compressive strength of the rock was measured to be 37.909 MPa, while the rock integrity index provided by the geological survey report was 0.44 and the rock wave speed was 3.42 km/s. In this paper, research results from the literature [27] are used to determine the deformation modulus of the rock mass, which is calculated by Equation (1).

$$E_m = \begin{cases} \left(\frac{1+K_v}{2}\right)\sqrt{\frac{\sigma_c}{100}} \cdot 10^{\left(\frac{15V_p-17.5}{40}\right)}, (\sigma_c \le 100\text{ MPa}) \\ \left(\frac{1+K_v}{2}\right) \cdot 10^{\left(\frac{15V_p-17.5}{40}\right)}, (\sigma_c > 100\text{ MPa}) \end{cases} \quad (1)$$

where E_m is the deformation modulus of the rock mass; σ_c is the uniaxial compressive strength of intact rock masses; K_v is the rock integrity index; and V_p is the rock body wave speed.

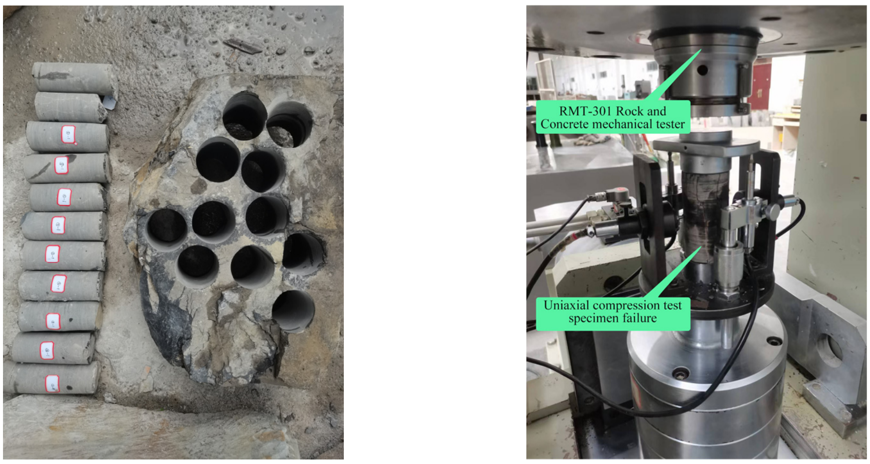

(**a**) (**b**)

Figure 3. Indoor rock test: (**a**) rock samples for testing; (**b**) rock uniaxial compression test.

Finally, the deformation modulus of the medium fractionated limestone is estimated to be 3.75 MPa. Combined with the field monitoring data and the experience of metro construction in the Guiyang area, the deformation modulus of this paper is taken as 2 MPa. The cohesion and internal friction angle of the rock layer and other parameters of the soil layer are taken from the geological survey report and the experience of metro construction in the Guiyang area.

The main mechanical properties of the strata are listed in Table 1. The thickness of the soil strata shown in Table 1 is the thickness of the soil strata at the time of modeling. Since the actual stratum is not a homogeneous stratum, the stratum thickness is taken as the average thickness of the actual stratum for the simplification of numerical modeling.

Regarding the swelling angle of the soil, the empirical formula is as follows: swelling angle = internal friction angle −30°. When the internal friction angle is less than 30°, the expansion angle can be regarded as close to 0°. Therefore, the swelling angle of the soil is not considered in this paper. Soil cohesion is denoted by c, and the angle of internal friction by φ. Standard statistical values for the consolidation of fast shear tests were used according to the ground investigation report.

Table 1. Main physical and mechanical parameters of the stratum.

Stratigraphic Name	Depth (m)	γ (kN/m^3)	E_m (GPa)	μ	c (kPa)	φ (°)
Miscellaneous fill	5.6	19	0.006	0.3	8	17
Red clay	1.4	17.76	0.015	0.35	40	10
Medium-weathered limestone	-	27.1	2.0	0.26	450	40
Rock surrounding reinforcement area	2.0	27.1	4.0	0.26	650	60

Note: γ is the stratum unit weight; E_m is the deformation modulus; μ is Poisson's ratio; c is cohesion; and φ is the angle of internal friction.

3. Pile Foundation Underpinning Program

3.1. Construction Scheme of Pile Foundation Underpinning

As Guiyang Rail Transit Line 3 crosses the bridge piles of Guihuang elevated bridge, some of the original bridge piles are truncated by the tunnel. In order to ensure the structural and operational safety of the Guihuang Viaduct, the pile foundations of piers 15 and 16 of the Guihuang Viaduct need to be underpinned. The construction solution is to use passive underpinning. The plan for the underpinned pile foundation is shown in Figure 4. A total of six bridge piles within the upstream and downstream lanes need to be underpinned; the piles to be underpinned are 15-5, 15-6, 16-1, 16-2, 16-4, and 16-5 of the Guihuang Viaduct, and the diameter of the pile to be replaced is 1.8 m, which is cast with C30 steel concrete. The diameter of the underpinning pile is 1.5 m, with a total of 16 piles. There are four underpinned bearing platforms, and both the underpinned bearing platform and underpinning pile are cast with C35 reinforced concrete. A total of three foundation pits are excavated, to an excavation depth of 5.4 m, from Huaguoyuan West Station to Huaguoyuan East Station in the direction of construction. The relationship between stratigraphy and pile foundation location and the profiles of the underpinning pile foundations 1-1, 2-2, and 3-3 are shown in Figure 5 (unit: cm).

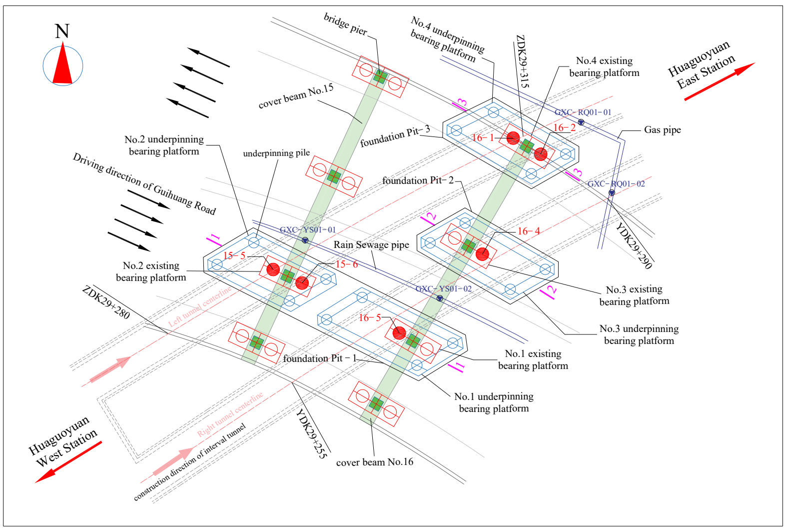

Figure 4. Pile buttress replacement plan location.

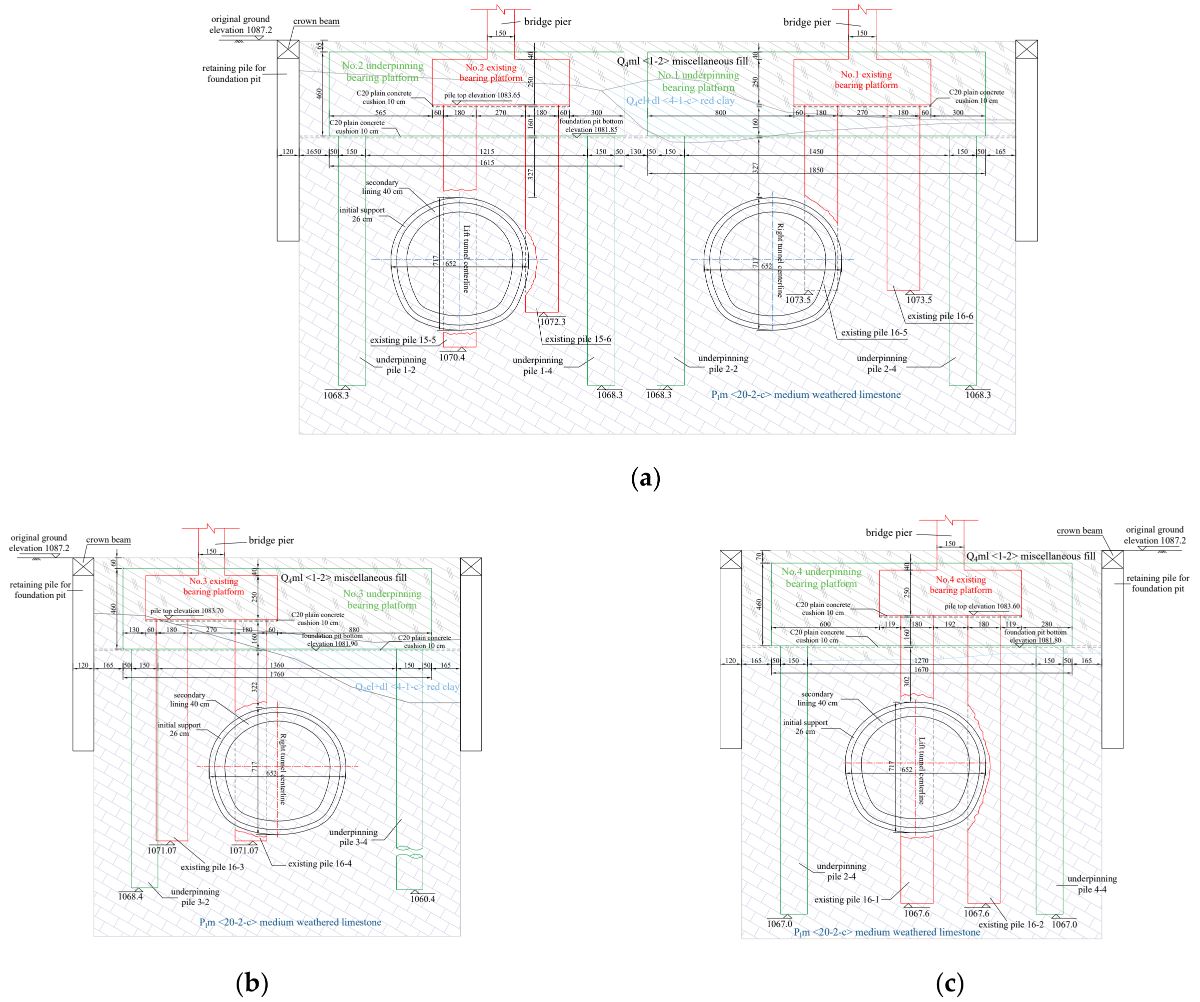

Figure 5. Underpinned pile foundation cross-section diagram: (**a**) Section 1-1; (**b**) Section 2-2; and (**c**) Section 3-3.

The construction process of the underpinned pile foundation is divided into a total of six construction stages, with the following construction steps: (1) underpinned pile and retaining pile for foundation pit construction; (2) the excavation of the foundation pit, pouring a 10 cm C20 concrete bedding layer at the bottom of the foundation pit, and welding connection steel on the side of the existing pile cap; (3) the underpinning pile cap is cast with C40 concrete; (4) in the underpinned bearing platform bottom, the local excavation of a 0.3 m~0.5 m deep trench, the wire saw cutting of the existing pile into a working surface, using the mechanical vibrationless linear cutting process to cut the existing pile, and backfilling the trench at the bottom of the platform with mortar; (5) backfilling the foundation pit to the original ground level, restoring the surrounding ground and road surface; and (6) tunnel construction, breaking up the existing pile foundation when encountered. These steps are shown in Figure 6.

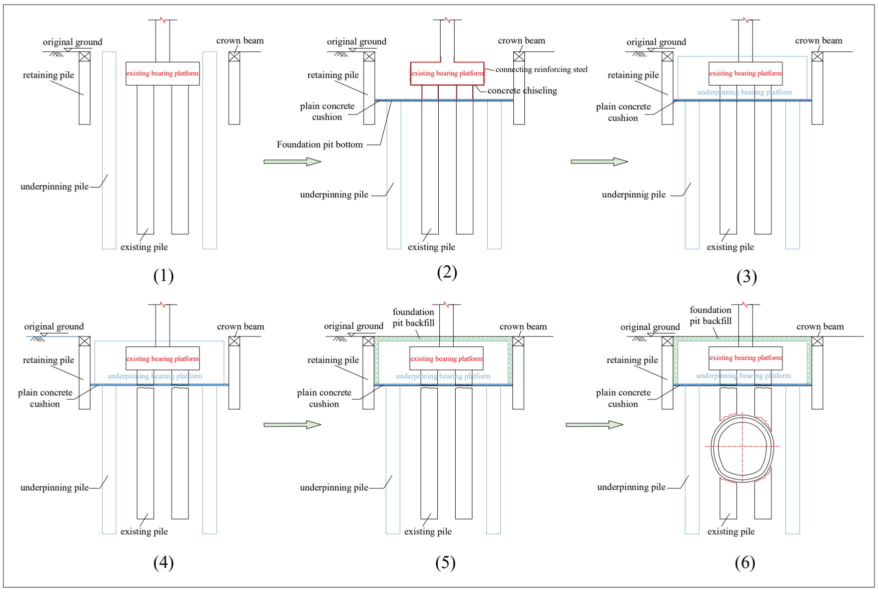

Figure 6. Underpinned pile foundation step diagram. (The serial number in the figure corresponds to the step sequence of pile foundation underpinning construction).

3.2. Analysis of Technical Difficulties

(1) The pile foundation underpinning section is very dense around the viaduct, and the location of the underpinning pile has invaded Guihuang Road. The process needs to occupy Guihuang Road into and out of the city-direction lanes for semiclosed construction.

(2) The location of the underpinning pile is close to the original bearing platform of Guihuang elevated bridge, which is an operational bridge. The bridge settlement and deformation control requirements during construction are high, and the disturbance to the old bearing platform during underpinning pile construction should be reduced by as much as possible.

(3) The foundation pit is surrounded by a rain–sewage pipeline and gas pipeline (as shown in Figure 4), and the construction may cause a large differential settlement of these pipelines, which may lead to the destruction of the pipelines.

(4) The process of underpinning the pile foundation is not completed at once, requiring multiple excavations and pile foundation truncation construction, which has a more complex impact on the settlement and deformation of the bridge structure.

4. Three-Dimensional Numerical Model

4.1. Finite Element Calculation Model

In this paper, the effects of underpinned pile foundation and tunnel construction on the existing elevated bridge were simulated using the 3D finite element analysis software Midas GTS. In order to simplify the model and weaken the influence of tunnel boundary effects on the simulation results, the dimensions of the model strata were calculated using 3 to 5 times the tunnel excavation diameter: longitudinal (80 m) $\times$ transverse (80 m) $\times$ vertical (50 m). The mesh used in this numerical model consists of 57,555 nodes and 94,142 elements. For the accuracy of calculation, the grid size of the tunnel excavation, pile foundation, and bearing platform area is divided by local encryption. Fixed constraints are added to limit the displacement of the model in the horizontal and bottom directions, while the upper part of the model has a free boundary without the addition of constraints. The lane loads were applied to the bridge deck, the same as they were to the uniform and concentrated loads, while RZ directional restraints were added to all pile foundations to limit their rigid body rotation displacement. The spatial dimensions of the computational model are shown in Figure 7a, and the internal schematic of the computational model is shown in Figure 7b.

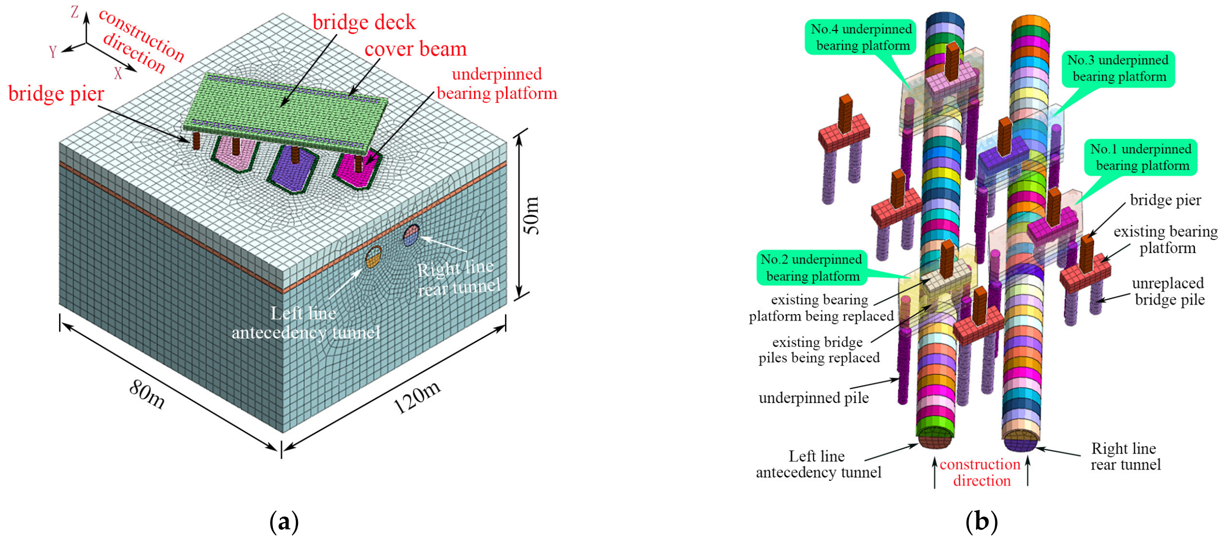

Figure 7. Schematic diagram of the computational model: (**a**) 3D spatial dimensions; (**b**) internal schematic diagram of the model.

4.2. Finite Element Calculation Parameters

In this paper, the geotechnical body adopts the Mohr–Coulomb yielding criterion as the intrinsic model [28], and the strata are divided into a total of three layers, all of which are assumed to be ideal elastic materials. The simulation of the bridge superstructure is simplified to a bridge slab, which is convenient for the analysis of the bridge deck settlement later. The simulated cover beam is a plate unit, and both the existing bearing platform and underpinning pile cap are simulated as solid units. A one-dimensional beam unit is used to simulate bridge piers, existing piles, and buttress piles. The advantage of the beam unit is that the pile–soil coupling can be ensured while the contact coefficient between piles and soil does not need to be set. According to the stiffness equivalence principle, the simplified foundation pit enclosure pile is an underground continuous wall, and the underground continuous wall and the initial support are simulated by the shell unit. The tunnel undercrosses Guihuang Viaduct in the level III surrounding rock, using Φ159 advanced pipe shed and grouting as presupport, and in the tunnel support system, the difference in stiffness between the anchor and the surrounding rock is large. The role of the anchor rod is mainly to improve the continuity and integrity of the surrounding rock, limiting the development of the surrounding rock plastic zone. In order to simplify the model, in this paper, the C and φ values and deformation modulus E_m of the surrounding rock around the tunnel are increased to form a surrounding rock reinforcement zone to simulate the effect of advanced pipe shed support when conducting numerical simulations. The physical and mechanical parameters of the surrounding rock reinforcement zone are shown in Table 1. The calculated model material parameters are shown in Table 2.

4.3. Numerical Simulation Process

The numerical simulation process is divided into three main stages: (1) the construction of Guihuang elevated bridge; (2) the construction of the underpinned pile foundation; and (3) the construction of the internal tunnel. In this paper, we mainly study the influence of the underpinning pile foundation and tunnel construction throughout the process of the settlement of existing elevated bridges, without considering the influence of existing elevated bridge construction; therefore, the displacement caused by the construction of Guihuang Viaduct is cleared.

Table 2. Material parameters of the computational model.

Material Type	Concrete Grade	E (GPa)	μ	γ (kN/m³)
Cover beam	C50	34.5	0.2	23.5
Bridge panel	C40	32.5	0.2	23.5
Underpinned bearing platform; underpinned pile	C35	31.5	0.2	23.5
Existing pile; existing bearing platform	C30	30	0.2	23.5
Bridge pier; underground continuous wall	C30	30	0.2	23.5
Initial support	C25	29	0.2	23.5
Foundation pit concrete backfilling	C20	25.5	0.2	23.5

Note: The parameters in the table are the same as above except that E represents the modulus of elasticity.

According to the actual construction situation on site, construction is divided into a total of 17 stages to simulate the whole construction process of the interval tunnel crossing the existing bridge foundation. The main construction steps are as follows: (0) construction of the diaphragm wall and underpinning piles; (1) foundation pit 1 excavation; (2) No. 1 and 2 underpinning platform construction; (3) No. 15-5, 15-6, and 16-5 existing piles cut off; (4) foundation pit 1 backfill; (5) foundation pit 2 excavation; (6) No. 3 underpinning platform construction; (7) No. 16-4 existing piles are cut off; (8) foundation pit 2 backfill; (9) foundation pit 3 excavation; (10) No. 4 underpinning pile cap construction; (11) No. 16-1 and 16-2 existing piles are truncated; (12) foundation pit 3 backfill; (13) tunnel construction (left line first, staggered construction of two tunnels, left and right line tunnels face staggered distance of 36 m; during the tunnel construction process, the construction step length of the surrounding rock reinforcement area is 2 m, and the step length is 2 m), close to the existing piles of the viaduct; (14-15) the tunnel passes through the bridge pile foundation and the barrier pile is removed; and (16) tunnel construction, away from the existing bridge pile foundation area.

4.4. Numerical Model Loads

(1) Self-weight

The self-weight coefficient of the calculation model is taken as g = 9.81 m/s^2 (because the tunnel burial depth is not large, the influence of the tectonic stress field is small, and the ground stress field is considered using the self-weight stress field).

(2) Bridge superstructure loading

The superstructure load is the main factor causing the structure to settle during the construction period. In this project: the bridge reinforced concrete and prestressed concrete unit weight is 26 kN/m^3, and the left and right deck of the second-phase paving take the value of 107.3 kN/m. In order to simplify the calculation, the superstructure load of the bridge is converted to the self-weight of the bridge deck slab (concrete grade C40).

(3) Lane load

The automobile design load of Guihuang Road Viaduct is calculated according to the City—Class A load, where the automobile load includes the lane load and vehicle load. This paper aims to calculate and analyze the overall structure of the bridge, so the lane load is used. Referring to the relevant provisions of the national standard “Code for design of urban bridges” (CJJ11-2011), the lane load is composed of concentrated load and uniform load, the standard value of the uniform load is taken as q_K = 10.5 kN/m, and the concentrated load is taken as PK = 302 KN.

5. Numerical Simulation Result Analysis

5.1. Verification of the Numerical Model

In order to verify that the established numerical model is reasonable and reliable, numerical simulation results and field monitoring data were compared for the settlement of the foundation pit enclosure (ground connection wall) and the settlement of bridge piers at different construction stages. In the bridge pile foundation underpinning construction site monitoring, the models Trimble-Dini0.3-748408 digital level (measurement accuracy of 1 mm) and LeicaTS09plus-1890787 total station (measurement accuracy of 1 mm) were used to monitor the foundation pit enclosure structure and bridge pier settlement.

It can be seen from Figure 8 that the measured data in the field of the foundation pit enclosure structure and the calculated results of numerical simulation are in the range of the settlement control requirements (<20 mm), so the numerical simulation results of this paper are reliable.

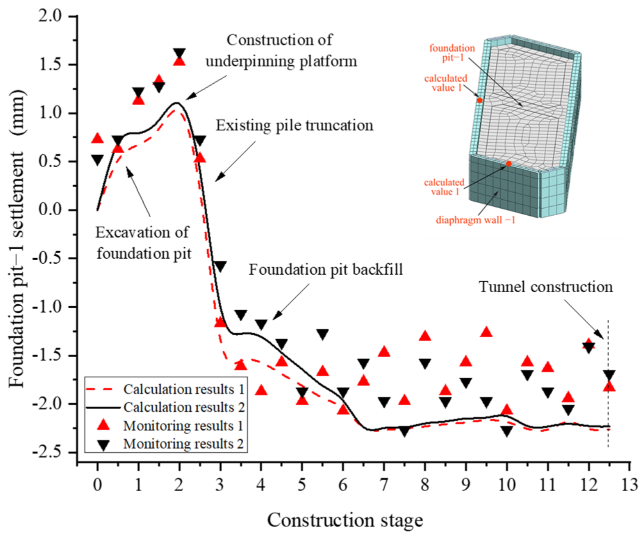

Figure 8. Diaphragm wall settlement curve.

The settlement variation curve of the bridge pier monitoring is shown in Figure 9b. From the figure, we can see that the maximum settlement of the bridge pier appears in pier 2, at 2.72 mm (<8 mm); the uplift of the bridge pier occurs at the foundation pit excavation, with a maximum value of 0.73 mm; and the settlement of the bridge pier meets the monitoring requirements. Overall, the numerically simulated bridge pier settlement is close to the monitoring results, which further indicates that the numerical simulation results in this paper are reliable.

5.2. Settlement Analysis of Foundation Pit Enclosure Structure

The settlement curve of the underground diaphragm wall with the construction process of pile foundation underpinning is shown in Figure 8 (this paper only takes foundation pit 1 as an example). From the figure, we can see that with the excavation of foundation pit 1, the underground diaphragm wall produces uplift, and the maximum amount of uplift is 1.2 mm. Underpinning bearing platform construction, existing pile truncation construction, foundation pit backfill, and other stages will cause the settlement of the diaphragm wall, with a maximum settlement amount of 2.2 mm. The settlement of the diaphragm wall slowly stabilized when the tunneling was carried out after the completion of the underpinning system.

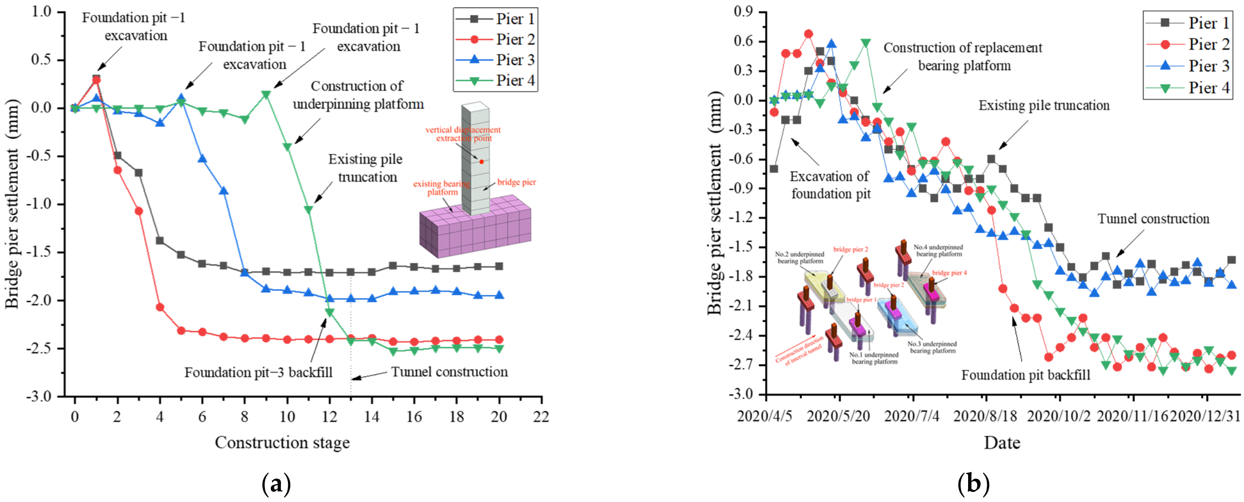

Figure 9. Settlement of bridge piers at different construction stages: (**a**) calculated value; (**b**) measured value.

5.3. Bridge Superstructure Deformation Characteristics

(1) Settlement analysis of bridge piers

As shown in Figure 9a, the vertical deformation of the bridge pier caused by each construction stage is analyzed (where pier 1 indicates the pier corresponding to the No. 1 underpinning bearing platform, as shown in Figure 4). It can be seen from the figure that the excavation of the foundation pit causes the piers to bulge, with a maximum bulge of 0.3 mm (occurring during the foundation pit 1 excavation phase). During the construction stage of the underpinning bearing platform, the settlement of the bridge pier was caused by the self-weight of the underpinning bearing platform, and the maximum settlement was 0.64 mm (bridge pier No. 2). During the existing pile truncation construction stage, the lower pile bearing capacity suddenly reduced, which caused the bridge superstructure to deform, and then the underpinning structure system transformation was completed, in which the existing pile truncation construction caused a large change in pier settlement. The settlement of piers 1, 2, 3, and 4 caused by the existing pile truncation construction stage accounted for 41%, 42%, 43%, and 43% of the total construction stage settlement, respectively. During the tunnel construction phase, the settlement of piers 1, 2, 3, and 4 was stabilized at around 1.6 mm, 2.4 mm, 1.9 mm, and 2.5 mm, respectively, which can be seen to have little effect on the bridge superstructure during this phase.

Four piers showed the same settlement trend, among which the superstructure loads of piers 1 and 3 were mainly shared by the underpinning system (underpinning bearing platform and underpinning pile) and the existing piles that were not truncated, so the settlement was smaller, being only 1.98 mm. The existing pile foundation corresponding to pier 2 and 4 needs to be truncated completely, and the entire upper load is transferred to the underpinning bearing platform and underpinning pile, so the settlement value is greater compared with pier 1 and 3. The maximum settlement value appeared in pier 4, with a value of 2.55 mm (<8 mm), meeting the settlement control requirements.

(2) Deformation analysis of the bridge deck

Similarly to Figure 10, which shows the settlement of the bridge deck during the construction of the underpinning pile foundation, it can be seen from Figure 9a that the diaphragm wall and the underpinning pile construction have minimal impact on the superstructure of the bridge; this is therefore not repeated below. From Figure 10b, it can be seen that soil loss during foundation pit excavation causes soil rebound inside the foundation pit, which drives the uplift deformation of the superstructure, and the maximum uplift of the bridge deck is approximately 0.37 mm; as can be seen in Figure 10c, when the underpinning bearing was poured, the new bearing settled under its own weight and the maximum settlement of the bridge deck was approximately 0.6 mm. From Figure 10d, it can be seen that the existing pile truncation construction leads to the direct transfer of the superstructure load to the underpinning bearing platform, and that due to the loss of the original pile bearing capacity, the settlement of the bridge deck becomes dramatically large, with a maximum settlement of 2.55 mm. From Figure 10e,f, it can be seen that the backfilling of the foundation pit (equivalent to soil loading) further causes a slow increase in superstructure settlement after the completion of the underpinning system, while the tunnel construction phase has almost no effect on the superstructure. The final settlement of the bridge deck was approximately 3 mm maximum (<8 mm), which satisfied the settlement control requirements.

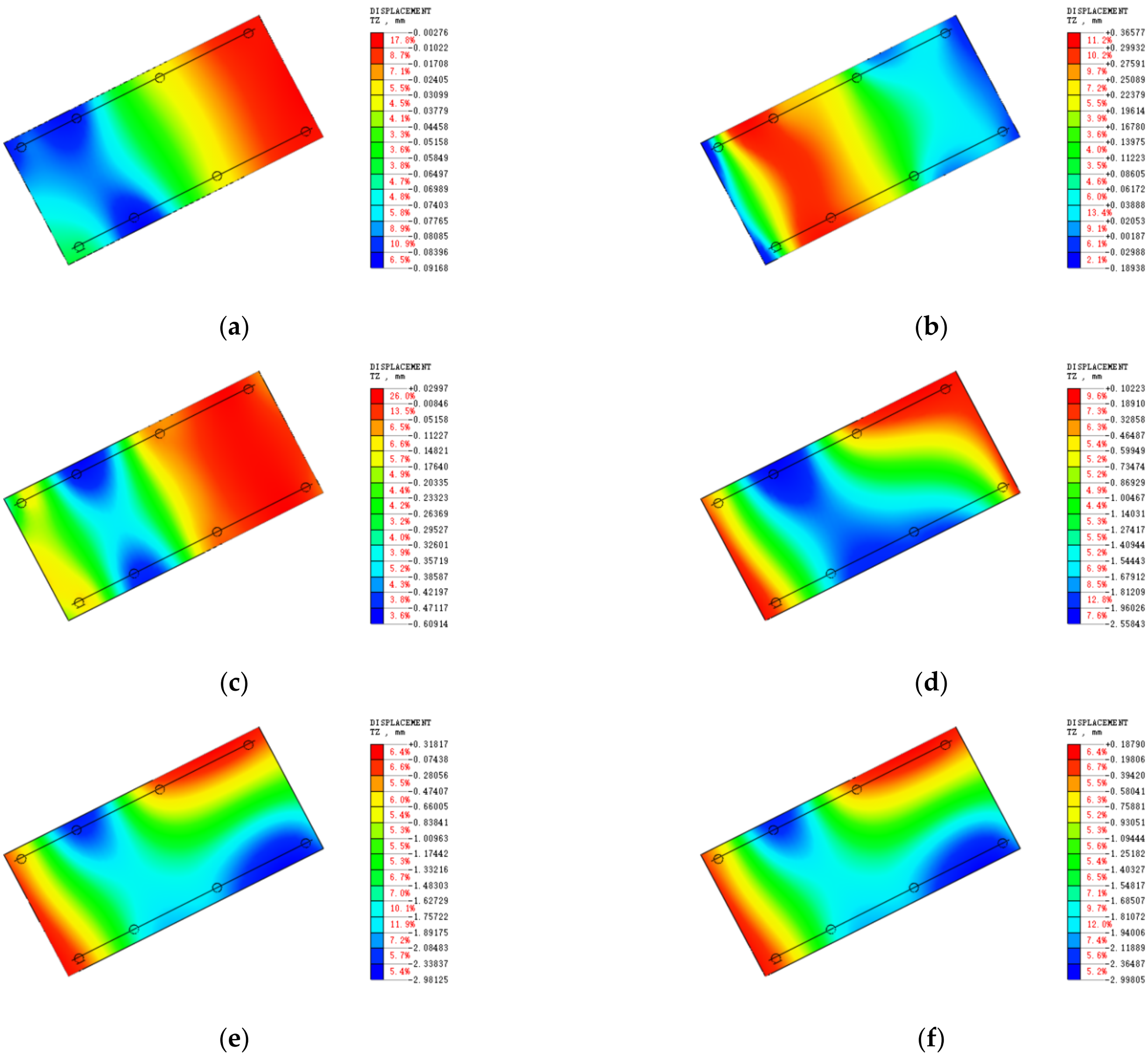

Figure 10. Major construction phases of bridge deck settlement: (**a**) diaphragm wall, underpinning pile construction; (**b**) foundation pit excavation; (**c**) underpinning bearing platform construction; (**d**) existing pile truncation; (**e**) foundation pit backfill; and (**f**) tunnel construction.

(3) Analysis of the monitoring results of surrounding pipelines

Due to the existence of a large number of pipelines around the foundation pit, the pile foundation underpinning and tunnel construction may cause a large differential settlement of the pipelines, which may lead to damage to the pipelines. In this project, the gas pipeline and rain–sewage pipeline near the foundation pit (as shown in Figure 4) were monitored using a digital level (measurement accuracy of 1 mm) of the model Trimble Dini0.3-748408. As shown in Figures 11 and 12, the maximum settlement of the rain–sewage pipe is 3.85 mm, and the maximum settlement of the gas pipe is 5.27 mm. The maximum differences in the settlement of the rain–sewage pipe and gas pipe are 0.25% Lg and 0.3% Lg, which both meet the monitoring control value (Lg indicates the length of the pipe section; L indicates the distance from the center of the adjacent foundation).

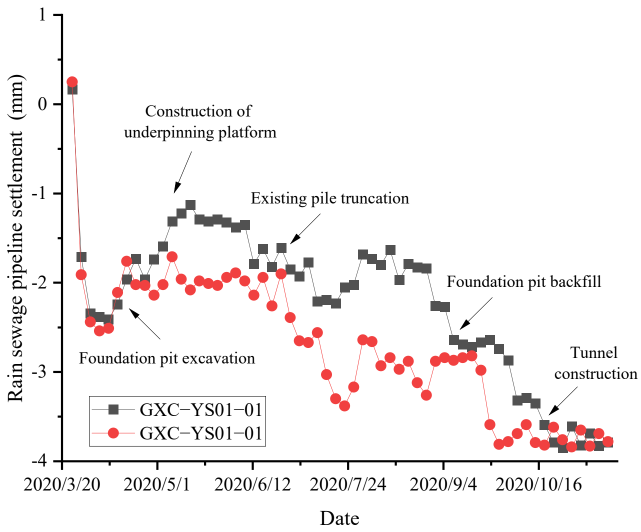

Figure 11. Settlement change curve of the rainwater and sewage pipeline.

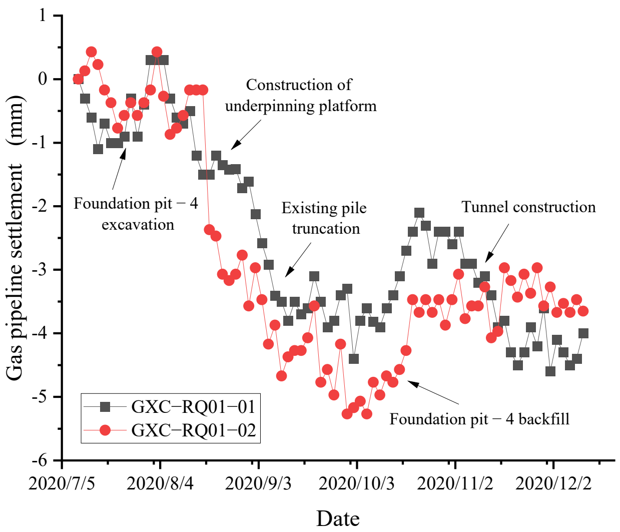

Figure 12. Settlement change curve of the gas pipeline.

5.4. Deformation Force Analysis of Existing Piles

As can be seen from above, the most significant impact on the deformation of the bridge superstructure during the construction of the pile foundation underpinning is the truncation phase of the existing piles. It is essential to study the deformation and axial force changes during the truncation of existing piles. Since the existing piles in this paper are mainly located in medium-weathered limestone, which can limit the displacement of the piles in the horizontal direction, this paper focuses on the vertical displacement of existing piles. We take the 16-3 (uncut) and 16-4 (cut) existing piles as an example to compare the deformation law of existing piles without underpinning and with underpinning construction. Taking the 16-5 and 16-1 existing piles as an example, we also compare the deformation and force change law of existing piles when underpinning one existing pile and underpinning two existing piles.

(1) Settlement analysis of existing piles 16-3 and 16-4

From Figure 13a, it can be seen that the settlement values of the pile tops of the existing pile 16-3 (untruncated) in the excavation of foundation pit 2, the construction of the underpinning bearing platform, the construction of the truncated existing pile, and the backfilling of foundation pit 2 are 0.1 mm, −0.55 mm, −1.22 mm, and −1.58 mm, respectively. The pile end settlement values are 0.13 mm, −0.49 mm, −1.15 mm, and −1.42 mm, respectively. The pile settlement is continuously varying; the settlement at the top of the pile is greater than the settlement at the end of the pile because it is in the upper-soft and lower-hard stratum (miscellaneous fill and medium-weathered limestone). The 16-3 existing pile settlement changes the most in the existing pile truncation construction stage; this stage of settlement accounts for 0.42% of the total settlement. From Figure 13b, it can be seen that the settlement change in the existing pile (truncated) No. 16-4 in the excavation stage of foundation pit 2 and the construction stage of the underpinning bearing platform is similar to that in Figure 13a, while in the construction stages of the truncation of the existing pile, the backfilling of foundation pit 2, and the breaking of the upper and lower step pile foundation, etc., the settlement change in the pile is discontinuous and can be divided into two parts from the truncated position of the existing pile, with settlement occurring at the top and uplift at the bottom. The maximum settlement of 1.81 mm occurs at the top of the pile. Comparing the maximum settlement of the existing piles in Figure 13a,b, the settlement of the truncated existing piles is slightly larger than the settlement of the untruncated existing piles, and uneven settlement occurs on both sides of the existing bearing platform.

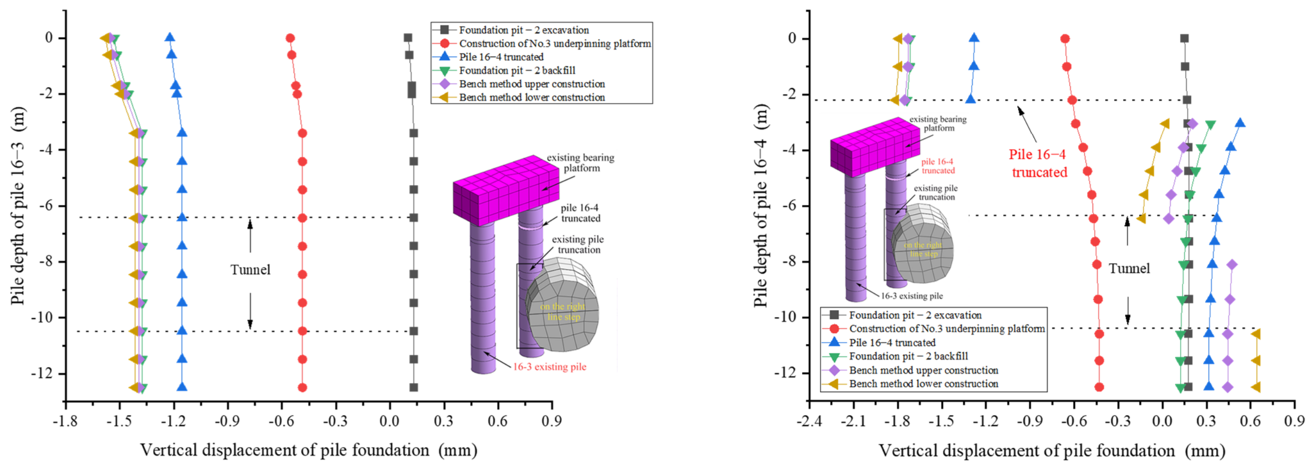

(**a**) (**b**)

Figure 13. Vertical settlement of existing piles at different construction stages: (**a**) pile 16-3 (untruncated); (**b**) pile 16-4 (truncated).

(2) Settlement analysis of existing piles 16-5 and 16-1

Comparing Figure 14a,b, it can be seen that the excavation phase of the foundation pit caused the upward displacement of the existing piles, with pile 16-5 bulging by approximately 0.35 mm and pile 16-1 bulging by approximately 0.2 mm; during the construction stage of the underpinning bearing platform, the existing piles settled under the self-weight of the underpinning bearing platform, and the settlement of the existing piles slowly decreased from top to bottom due to the action of pile side friction. The maximum settlement of the top of the existing pile is approximately 0.54 mm and the maximum settlement of the end of the existing pile is approximately 0.35 mm. With the truncation of the existing piles, the loss of bearing capacity at the end of the existing piles leads to the deformation of the superstructure; at this time, the upper load produces stress redistribution and is transferred to the underpinning structure, which mainly bears the upper structure load. The overall vertical displacement of the existing pile from the location of pile truncation can be divided into two parts: in the upper part, settlement occurs, with a 16-5 and 16-1 pile settlement of 1.45 mm and 1.82 mm, respectively; the lower part does not bear the upper load (equivalent to unloading) of the issued bulge, with a 16-5 and 16-1 pile bulge of 0.3 mm and 0.15 mm, respectively. In the foundation pit backfill stage, the upper part of the existing pile still bearing the load continues to produce settlement, with a 16-5 and 16-1 pile settlement of 1.81 mm and 2.37 mm, respectively, and the lower part of the existing pile no longer bears the load, which is slowly stabilized with a settlement amount close to 0. Then, pile foundation underpinning can be considered to be completed, with the upper part of the load having been transferred to the underpinning bearing platform and the underpinning pile. During the tunnel construction phase, the settlement of the existing piles stabilized when the tunnel passed through the barrier pile and was removed, with a maximum settlement of 2.46 mm (pile 16-1). The difference between the 16-5 and 16-1 existing pile settlements is large because the No. 4 existing bearing platform in the existing pile truncation needs to remove these two existing piles. The existing pile bearing capacity loss is greater; therefore, the settlement of the existing pile 16-1 is also even greater.

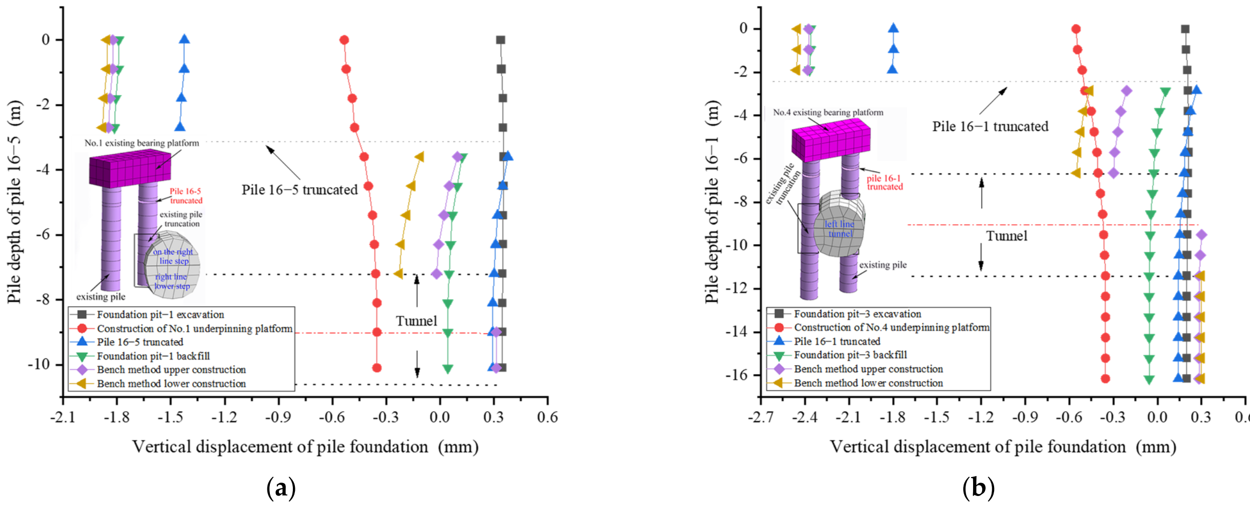

Figure 14. Vertical settlement of existing piles at different construction stages: (**a**) pile 16-5; (**b**) pile 16-1.

(3) Force analysis of existing piles 16-5 and 16-1

Figure 15 shows the axial force variation in the existing piles at different construction stages of piles 16-5 and 16-1. The analysis shows that before the truncation of the existing piles, the maximum axial forces at the top of piles 16-5 and 16-1 were 3536 KN and 3133 KN, respectively, and the maximum axial forces at the pile ends were 1466 KN and 1620 KN, respectively. The piles are located in better ground conditions, and the friction between the pile and soil reduces the pressure transmitted to the pile by the superstructure; therefore, the axial force of the existing pile gradually decreases with the increase in pile depth. Meanwhile, during pile truncation construction, the maximum axial force at the top of piles 16-5 and 16-1 is 2880 KN and 2583 KN, respectively, and it can be seen that the bearing capacity of the remaining pile foundation is smaller when both piles are underpinning. The load of the superstructure is transferred to the underpinning bearing more strongly at this time. The pile foundation below the truncated part does not bear the upper load, so the axial force is reduced and tends to zero. The axial force of the existing piles did not change significantly during the construction of the interval tunnel and the removal of the barrier piles, which also indicates that the tunnel construction has little impact on the superstructure of the bridge after the construction of the pile foundation underpinning is completed.

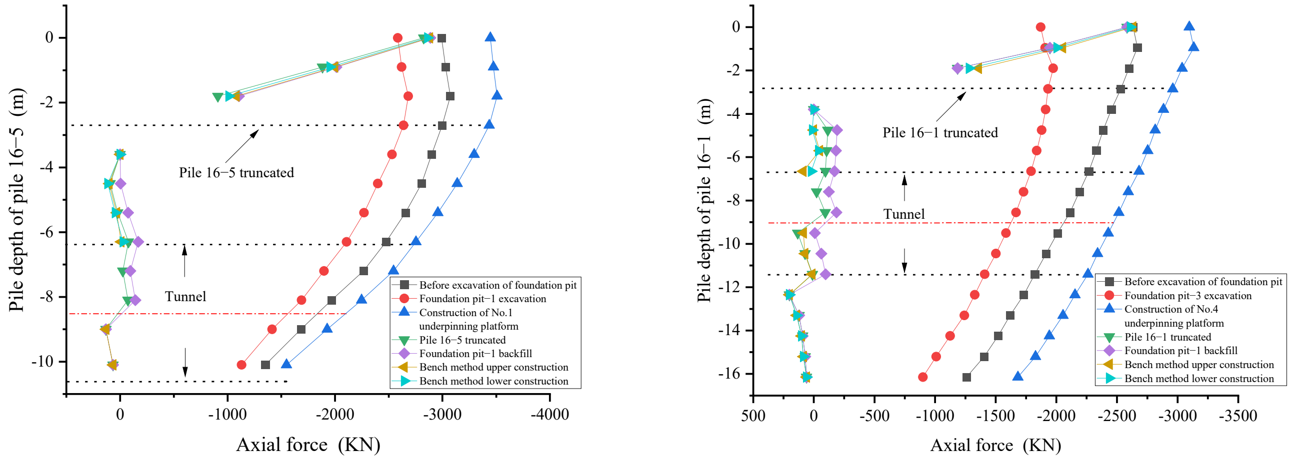

(**a**) (**b**)

Figure 15. Axial forces of existing piles at different construction stages: (**a**) pile 16-5; (**b**) pile 16-1.

5.5. Deformation Force Analysis of Bearing Platform

(1) Settlement analysis of existing bearing platform

Figure 16 gives the settlement curves of the two ends of the existing bearing platform at different construction stages, where P1 and P2 are the settlement of the two ends of the existing bearing platform No. 3 (one existing pile truncated), and P3 and P4 are the settlement of the two ends of the existing bearing platform No. 4 (two existing piles truncated). It can be seen that for P1 and P2 during existing pile truncation construction, the ends of the No. 3 existing bearing platform generated uneven settlement. The bearing platform was tilted to the end of the existing truncated pile, which at this time was not conducive for the existing bearing platform to transfer the upper load to the underpinning bearing platform. The settlement curves of P3 and P4 basically overlap, indicating that the settlement of the existing bearing platform No. 4 is uniform, and it is more favorable for the existing bearing platform to transfer the upper load to the underpinning bearing platform. However, the settlement of the No. 4 existing bearing platform is slightly larger than that of the No. 3 existing bearing platform. In general, the settlement law of the existing bearing platform is similar to the settlement law of the bridge pier in each construction stage.

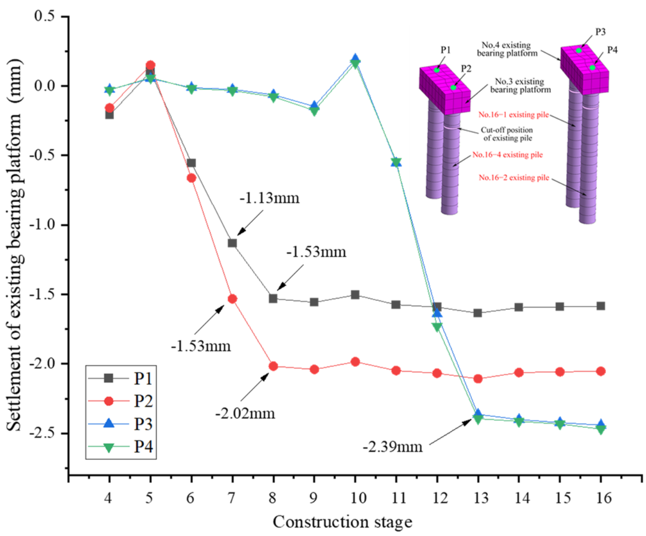

Figure 16. Settlement curves of existing bearing platform at different construction stages.

(2) Force analysis of underpinned bearing platform

After the underpinning structure system transformation is completed, the superstructure load is mainly borne by the underpinning bearing and is transferred to the underpinning piles. As shown in Figure 17, the diagram shows the tensile stresses applied to the underpinning bearing platform at each stage of construction (damage to concrete occurs predominantly through tensile damage).

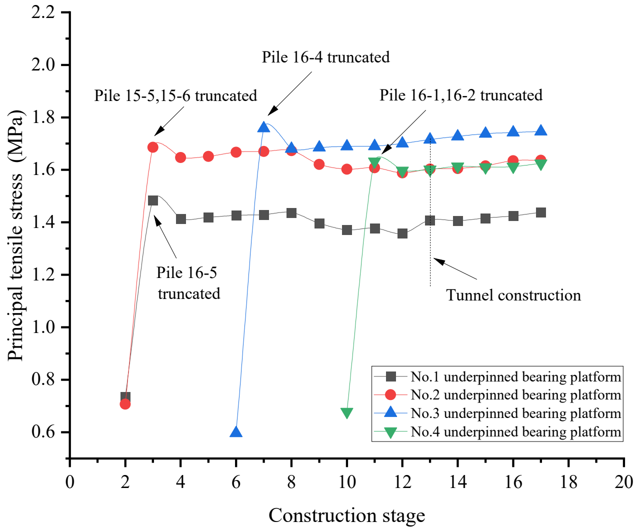

Figure 17. Maximum tensile stress of underpinned bearing platform at different construction stages.

As can be seen from Figure 17, the underpinning structure began to work after the completion of the truncated construction phase of the existing piles, under the joint action of the upper load and the uneven settlement of the existing bearing platform. There was a sharp increase in the local maximum tensile stress of the underpinning bearing platform, with the local maximum tensile stress of the underpinning bearing platforms No. 1, 2, 3, and 4 being 1.48 MPa, 1.69 MPa, 1.76 MPa, and 1.63 MPa, respectively. The local maximum tensile stress of the underpinning bearing platform appears at the junction between the bearing and the pile foundation, and most of the area is below the design value of C35 concrete tensile strength of 1.52 MPa, except for a very small part of the area where the stress is concentrated (refer to the Design Specification for Highway Reinforced Concrete and Prestressed Concrete Bridges and Culverts (JTG 3362-2018)). After the completion of the pile foundation underpinning, the maximum tensile stress curve on the underpinning bearing platform during the tunnel construction phase changes smoothly, and tunnel construction can be considered to have no significant effect on the underpinning bearing platform.

6. Conclusions

This paper investigates the effect of using passive underpinning construction on existing bridges when undercrossing existing bridges in interval tunnels. The main findings are as follows:

(1) By combining numerical simulation and measured data, we compared the settlement of the foundation pit and bridge piers caused by the main construction stages. The numerical simulation results and the measured data results were consistent, which proves the accuracy of the numerical model.

(2) The settlement change law of the bridge deck is expressed as follows: the foundation pit excavation stage, equivalent to the foundation pit bottom unloading; the foundation pit bottom uplift drives the bridge superstructure to uplift; and the underpinning bearing platform construction, existing pile truncation, and foundation pit backfill stages cause the bridge deck to sink, with the existing pile truncation construction stage causing the largest settlement of the bridge deck, accounting for approximately 40% of the total settlement during the entire construction process. At the same time,

tunnel undercrossing construction removes obstacle piles, the impact on the bridge superstructure is very limited, and the settlement of the bridge deck tends to stabilize, so the impact of tunnel construction on the existing bridge can be ignored.

(3) Through the comparison of the settlement of existing piles requiring underpinning and existing piles not requiring underpinning in the same existing bearing, we found that the settlement of the truncated existing piles was larger than the settlement of the untruncated existing piles, which caused uneven settlement on both sides of the existing bearing platform. In the comparison of underpinning one existing pile and underpinning two existing piles, we found that the superstructure load of the former is shared by the existing pile without underpinning and the underpinning structure; the settlement of the latter is larger, and the superstructure is completely borne by the underpinning bearing and the underpinning pile.

(4) The settlement law of the existing bearing platform and that of the bridge pier are similar. Further analysis of the forces in the underpinning bearing reveals that the maximum tensile stress is generated during the truncated construction phase of the existing pile, with a maximum local tensile stress of 1.76 MPa. It appears at the junction of the existing bearing and existing pile, and most of the area is lower than the design value of C35 concrete tensile strength of 1.52 MPa. The reinforcement at the junction of the existing bearing and existing pile should be strengthened during construction to meet the safety requirements for the force of the underpinning bearing platform.

(5) When using passive underpinning and an underpinning bearing platform as construction solutions for underpinning the structures of pile foundations, the settlement of the upper bridge structure, the internal force of the underpinning bearing platform, and the settlement of the surrounding pipelines are all within safe ranges. It is therefore reasonable and feasible to use passive underpinning for similar projects.

Author Contributions: Conceptualization, Y.Z.; methodology, Y.Z. and Y.L. (Yuanming Liu); software, Y.Z.; validation, Y.Z. and Y.L. (Yuanming Liu); investigation, Q.C.; resources, Y.L. (Yuanming Liu); writing—review and editing, Y.Z.; visualization, X.O. and Y.L. (Yingxiao Li); supervision, Y.L. (Yuanming Liu). All authors have read and agreed to the published version of the manuscript.

Funding: This work is supported by the Guiyang Metro Line 3 Phase I Engineering Research Project (Project No. GD3-FW-YJ-05-2020-13-ZB, to Yuanming Liu), the Science and Technology Planning Project of Guizhou Province (Qiankehe Basic Project ZK [2022] General Project 082, Qiankehe Basic Project [2019] No. 1057, and Qiankehe Major Special Project [2018] 3011), and the Regional First-Class Discipline Construction Project in Guizhou Province (QYNYL [2017] 0013).

Institutional Review Board Statement: Not applicable.

Informed Consent Statement: Not applicable.

Data Availability Statement: Not applicable.

Acknowledgments: The authors gratefully acknowledge Wenrong Ma of China Railway Eighth Engineering Group Third Engineering Co., Ltd. and Xiaoyong He of China Railway Development Investment Group Co., Ltd. for their valuable comments and support. The authors also thank the reviewers and editors for their valuable comments and suggestions, which helped to improve the quality of the paper.

Conflicts of Interest: The authors declare no conflict of interest.

References

1. Ding, H.; Su, L.; Lai, J.; Zhang, Y. Development and Prospect of Root Piles in Tunnel Foundation Reinforcement. *Stavební Obz.—Civ. Eng. J.* **2017**, *26*, 250–266. [CrossRef]
2. Shan, H.; Xia, T.; Yu, F.; Tao, H.; He, S.; Giosuè, B.; Boscato, G. Influence of Underpinning Pile Drilling Construction on the Bearing Behavior of Existing Loaded Foundation Piles: Case Study. *Adv. Civ. Eng.* **2020**, *2020*, 9568279. [CrossRef]
3. Liang, F.; Cao, P.; Qin, H. Influence of excavation beneath existing building on dynamic impedances of underpinning pile considering stress history. *J. Cent. South Univ.* **2020**, *27*, 1870–1879. [CrossRef]

4. Marshall, A.M.; Haji, T. An analytical study of tunnel–pile interaction. *Tunn. Undergr. Space Technol.* **2015**, *45*, 43–51. [CrossRef]
5. Wang, K.; Wu, W.; Zhang, Z.; Leo, C.J. Vertical dynamic response of an inhomogeneous viscoelastic pile. *Comput. Geotech.* **2010**, *37*, 536–544. [CrossRef]
6. Xiang, Y.; Jiang, Z.; He, H. Assessment and control of metro-construction induced settlement of a pile-supported urban overpass. *Tunn. Undergr. Space Technol.* **2008**, *23*, 300–307. [CrossRef]
7. Jinyong, Z. Model Test Research on Underpinning Technology of Bridge Pile Foundation of Lanzhou Metro Line 1. *Urban Mass Transit* **2022**, *25*, 86–91.
8. Wang, C.; Han, J.; Jang, Y. Experimental Investigation of Micropile Stiffness Affecting the Underpinning of an Existing Foundation. *Appl. Sci.* **2019**, *9*, 2495. [CrossRef]
9. Yan, L.; Wang, G.; Chen, M.; Yue, K.; Li, Q. Experimental and Application Study on Underpinning Engineering of Bridge Pile Foundation. *Adv. Civ. Eng.* **2018**, *2018*, 5758325. [CrossRef]
10. Wang, X.; Wang, X.; Jiang, D.; Wang, Y. Study on Bearing Characteristics Model Test for Passive Underpinning System of Bridge Pile Foundation. *Railw. Eng.* **2018**, *58*, 51–54.
11. Wang, X. *The Shear Theory and Experiment Research of Pile Foundation Underpinning Based on the Truss—Arch Model*; Xi'an University of Architecture and Technology: Xi'an, China, 2017.
12. Zhang, L.; Li, Q.; Li, L.; Wang, X. Experimental study on shear bearing capacity of bond-interface between new and old concrete in underpinning engineering of high-loaded pile foundation. *J. Civ. Environ. Eng.* **2015**, *37*, 154–158.
13. Li, P.; Lu, Y.; Lai, J.; Liu, H.; Wang, K. A Comparative Study of Protective Schemes for Shield Tunneling Adjacent to Pile Groups. *Adv. Civ. Eng.* **2020**, *2020*, 6964314. [CrossRef]
14. Jia, Q.; Zhang, X.; Ying, H.Q. Numerical analysis of settlement difference for pile foundation underpinning for constructing underground space. *Rock Soil Mech.* **2009**, *30*, 3500–3504.
15. Wu, C.J.; Yu, F.; Gong, X.N.; Lin, C.G.; Liang, R.Z. Influence of excavation unloading on vertical bearing behavior of existing pile groups. *Rock Soil Mech.* **2014**, *35*, 2602–2608.
16. Song, N. Design and Construction of the Underpinning of a River-Crossing Bridge Pile Foundation in a Metro Tunnel. *Mod. Tunn. Technol.* **2013**, *50*, 164–169.
17. Huang, X.; Chen, H.; Yan, Q.X. Research on Pile Foundation Underpinning of Subway Running Tunnel Passing under Existing Bridge. *Railw. Stand. Des.* **2016**, *60*, 89–93.
18. Zhou, J. Construction Technology and Environmental Impact Prediction for a Shield Tunnel under a Viaduct Pile Foundation Group. *Mod. Tunn. Technol.* **2016**, *53*, 165–172.
19. Wang, Z.; Zhang, K.; Wei, G.; Li, B.; Li, Q.; Yao, W. Field measurement analysis of the influence of double shield tunnel construction on reinforced bridge. *Tunn. Undergr. Space Technol.* **2018**, *81*, 252–264. [CrossRef]
20. Dong, X. Case Study on Design of Underpinning of Foundation Piles of Yiguanmiao Overpass in Construction of Line 3 of Chengdu Metro. *Tunn. Constr.* **2015**, *35*, 821–827.
21. He, W.F. *The Application of Passive Pile Foundation Underpinning Project to Subway Construction*; South China University of Technology: Guangzhou, China, 2012.
22. Xu, Q.; Zhu, H.; Ma, X.; Ma, Z. Pile underpinning and removing technology of shield tunnels crossing through group pile foundations of road bridges. *Chin. J. Geotech. Eng.* **2012**, *34*, 1217–1226.
23. Zhang, C.; Zhao, Y.; Zhang, Z.; Zhu, B. Case Study of Underground Shield Tunnels in Interchange Piles Foundation Underpinning Construction. *Appl. Sci.* **2021**, *11*, 1611. [CrossRef]
24. Zhang, L. Study on Underpinning Scheme of Viaduct Pile Foundation Crossed by Shield Tunnel. *IOP Conf. Ser. Earth Environ. Sci.* **2020**, *570*, 52028.
25. Xu, Q.; Zhu, H.; Ma, X.; Ma, Z.; Li, X.; Tang, Z.; Zhuo, K. A case history of shield tunnel crossing through group pile foundation of a road bridge with pile underpinning technologies in Shanghai. *Tunn. Undergr. Space Technol.* **2015**, *45*, 20–33. [CrossRef]
26. Li, Z.; Chen, Z.; Wang, L.; Zeng, Z.; Gu, D. Numerical simulation and analysis of the pile underpinning technology used in shield tunnel crossings on bridge pile foundations. *Undergr. Space* **2021**, *6*, 396–408. [CrossRef]
27. Zhu, X.X.; Chen, C.X.; Xia, K.Z. Methods of Obtaining Mechanics Parameters of Rock Mass Based on Hoek-Brown Criterion. *J. Yangtze River Sci. Res. Inst.* **2015**, *32*, 111–117.
28. Wang, N.; Jiang, Y.; Geng, D.; Huang, Z.; Ding, H. Numerical Investigation of the Combined Influence of Shield Tunneling and Pile Cutting on Underpinning Piles. *Front. Earth Sci.* **2022**, *10*, 896634. [CrossRef]